Spring 2015

Design of a Horizontal Creep Testing Machine

Michael Presby
mjp80@zips.uakron.edu

The University of Akron

Design of a Horizontal Creep Testing Machine

Senior Design/Honors Research Project

Michael Presby

5-1-2015

Contents

Abstract

The design process for a horizontal creep testing machine is presented along with the material selection of grips for high temperature tensile tests. The design process consisted of creating multiple sketches of the testing machine in order to determine the best design to satisfy the given design parameters. The critical points of the frame were determined and derivations were performed in order to determine the maximum stress at the critical points and the maximum deflection due to the applied load. The information gathered from these derivations will be useful in comparing the two material choices for the frame which are aluminum structural framing and steel.

The material selection process for the grips was also presented. The material of choice for the grips must be able to withstand high temperature as well as have high strength and high stiffness. The economic side of choosing a material was also taken into account in order to determine the material that provides the best performance while minimizing cost. It was determined that the ideal material is silicon carbide and the best shaping process for a small batch size is to use conventional machining.

Introduction

A creep testing machine is used to measure the creep of a test specimen. Creep is the behavior of materials to deform at elevated temperatures and at a constant stress or load. Creep is important in determining how much strain (load) an object can handle in order to determine which material to use for a specific application.

The basic design of a creep testing machine is the support structure, the loading device (deadweight or actuator), the fixture device (grips and pull rods), and the furnace. The specimen being tested is held in place by the grips and a furnace surrounds the test section and maintains a constant temperature. The alignment of the test specimen is crucial to gather an accurate reading of the creep of the material. The load is transmitted to the test specimen via the fixture devices and the specimen is held in constant tension throughout the test.

Typical strain-curves obtained from creep tests exhibit three characteristic stages: primary creep, secondary creep, and tertiary creep. In the primary creep stage, the material initially deforms rapidly but the rate of deformation begins to decrease until it becomes constant. This constant creep strain rate is the secondary creep stage. Ideally, materials will stay in the secondary stage for relatively long periods of time. The final stage is the tertiary stage where the creep strain rate accelerates rapidly ultimately resulting in rupture. A typical strain-curve obtained from a creep-test is shown in Figure 1.

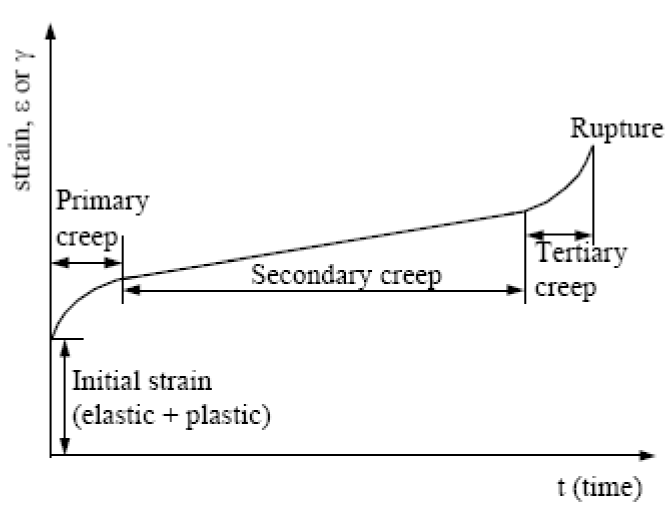

Figure 1. Typical strain-curve obtained from creep test

Creep can be measured using a vertical test machine or a horizontal test machine. In both cases, the specimen is held in a constant tensile load and subjected to a constant temperature. However, if one were to use a burner assembly to apply a flame directly to the test specimen, a horizontal test frame would be ideal. Compared to a vertical test frame, a horizontal frame prevents a chimney effect which results in a more precise application of the flame to the specimen. The design process of a horizontal test frame is developed and presented along with the material selection for the grips.

Design Criteria

Any machine that measures the creep of a material must be perfectly aligned in order to provide an accurate representation of the material's creep behavior. Therefore, the machine should have some sort of self-aligning mechanism. In addition, the test frame must be able to withstand any applied load. For this design, the maximum load that a test specimen will be subjected to will be 10kN. In order to provide a factor of safety, the design of the frame should be able to withstand between 15kN and 20kN.

Furthermore, the distance from the floor to the test specimen should be at a comfortable distance for the user to easily handle the test specimen and make any necessary adjustments. The frame should also allow the specimen to be visible from all sides in order to allow for observation and the use of cameras to record the test. The user should also have the capability to move additional test equipment such as a furnace, extensometer, cameras, etc. in and out of position easily. This can be accomplished by the use of a track system.

Additional design requirements include having space for a burner assembly and for the specimen to not travel far after rupture. Ideally, once the specimen ruptures, half of the specimen will be pulled out of the furnace. Table 1 displays the design criteria in order of importance for the test frame.

In addition to the design of the test frame, grips will also need to be designed and machined. The grips should be able to withstand high temperatures, must not fail or deflect too much under the design load, and have a minimal thermal expansion coefficient. Table 2 shows the translation for the material selection of the grips for high temperature tensile test.

Function	Creep Testing Machine
Design Criteria	Design load 15kN - 20kN
	Self-aligning mechanism
	Load applied using deadweight
	Half of specimen should pull out of furnace after rupture
	Track system for addition test equipment
	Distance from floor to specimen approximately 48"
	Specimen must be visible from all sides
	Space to slide burner assembly under specimen

Table 1. Design criteria for test frame

Function	Grip for high temperature tensile test
Constraints	Strength - must not fail under design load
	Stiffness - must not deflect too much under design load
	Withstand high temperature (max service temp ≥ 700°C)
	Minimal thermal expansion coefficient
Objective	Minimize cost
Free Variables	Choice of Material

Table 2. Translation for grips

Design Process for the Frame

The initial design process entailed observing other creep test machines and drawing multiple sketches. These sketches were then analyzed to see which ones best met the design criteria and the most suitable sketch was selected to move on in the design process.

Figure 2 shows a typical test area for a vertical tensile test. This test are uses hydraulic wedge grips as well as an aluminum track system to move the furnace into position once the specimen is positioned within the grips.

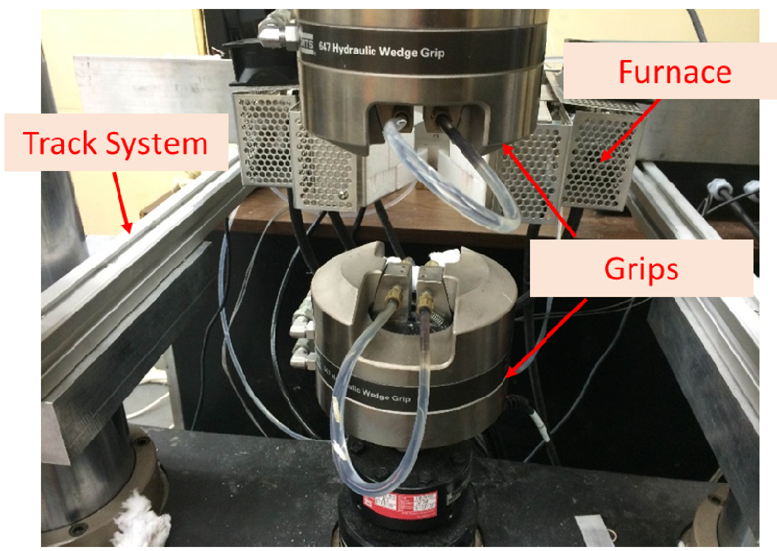

Figure 2. Vertical tensile test setup

Figure 3 illustrates how the extensometer is attached and moves using the aluminum track system. The track system is an important part of the frame design due to the extra test equipment that is necessary during a creep test.

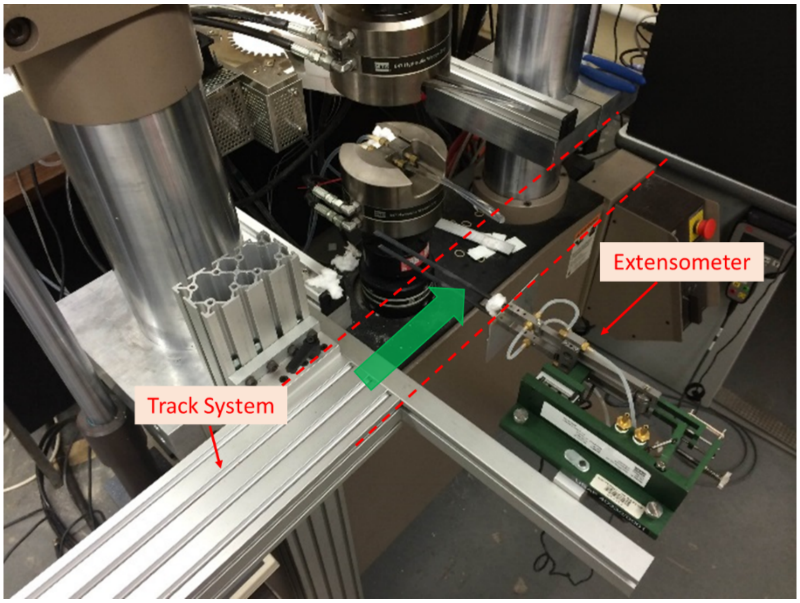

Figure 3. Track system and extensometer

The test machine shown in Figures 2 and 3 utilize an actuator to provide the load to the test specimen. The design for the horizontal test machine will use deadweight to provide a tensile load to the test specimen. Figure 4 shows an example of the setup of a deadweight loading system. The frame is made out of aluminum structural frame and also serves as its own track system for additional equipment.

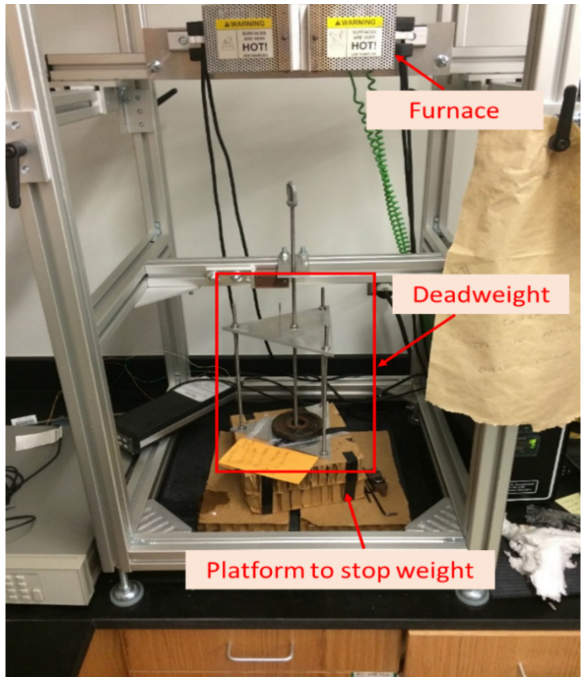

Figure 4. Vertical tensile test with deadweight loading system

The initial sketch for a horizontal creep testing machine is illustrated in Figure 5. The initial design incorporates a hydraulic actuator to apply the load and does not meet the design requirement that the test specimen must be visible from all sides for observation. In order to satisfy the requirement that the test specimen should be easily handled by the user at a height of approximately 48 inches, the test machine would have to be placed on a support fixture. In addition, this design incorporated a hydraulic actuator because the initial plan included two designs. It was later decided to primarily focus on a design incorporating deadweight.

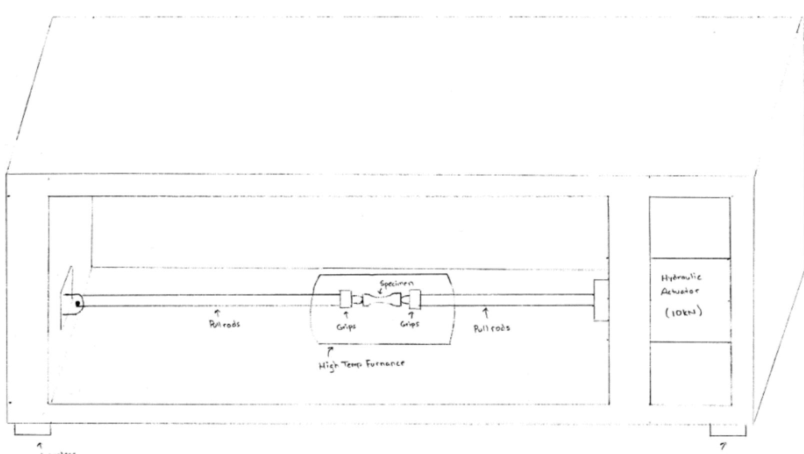

Figure 5. Initial design sketch

The design was updated following the initial sketch and is illustrated in Figure 6. This design featured a pulley system to transfer the load to the specimen. Due to the large amount of mass required to provide a force of 10 kN, the frame had two pulleys attached in order to have the mass located in the center of the test frame. This would allow for the center of gravity to remain approximately in the center of the test frame and therefore preventing any sort of moment (tipping force) that would need to be counterbalanced. The frame was redesigned to allow for full observation of the test specimen.

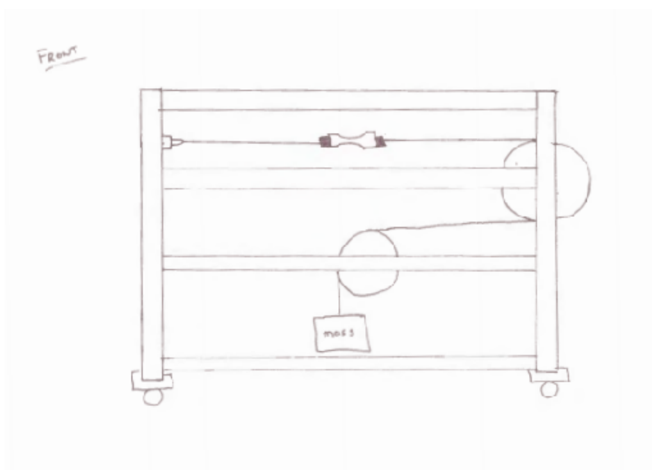

Figure 6. Second design sketch

Due to the possibility of implementing a burner assembly at a later time, an updated version of the test frame was designed and shown in Figure 7.

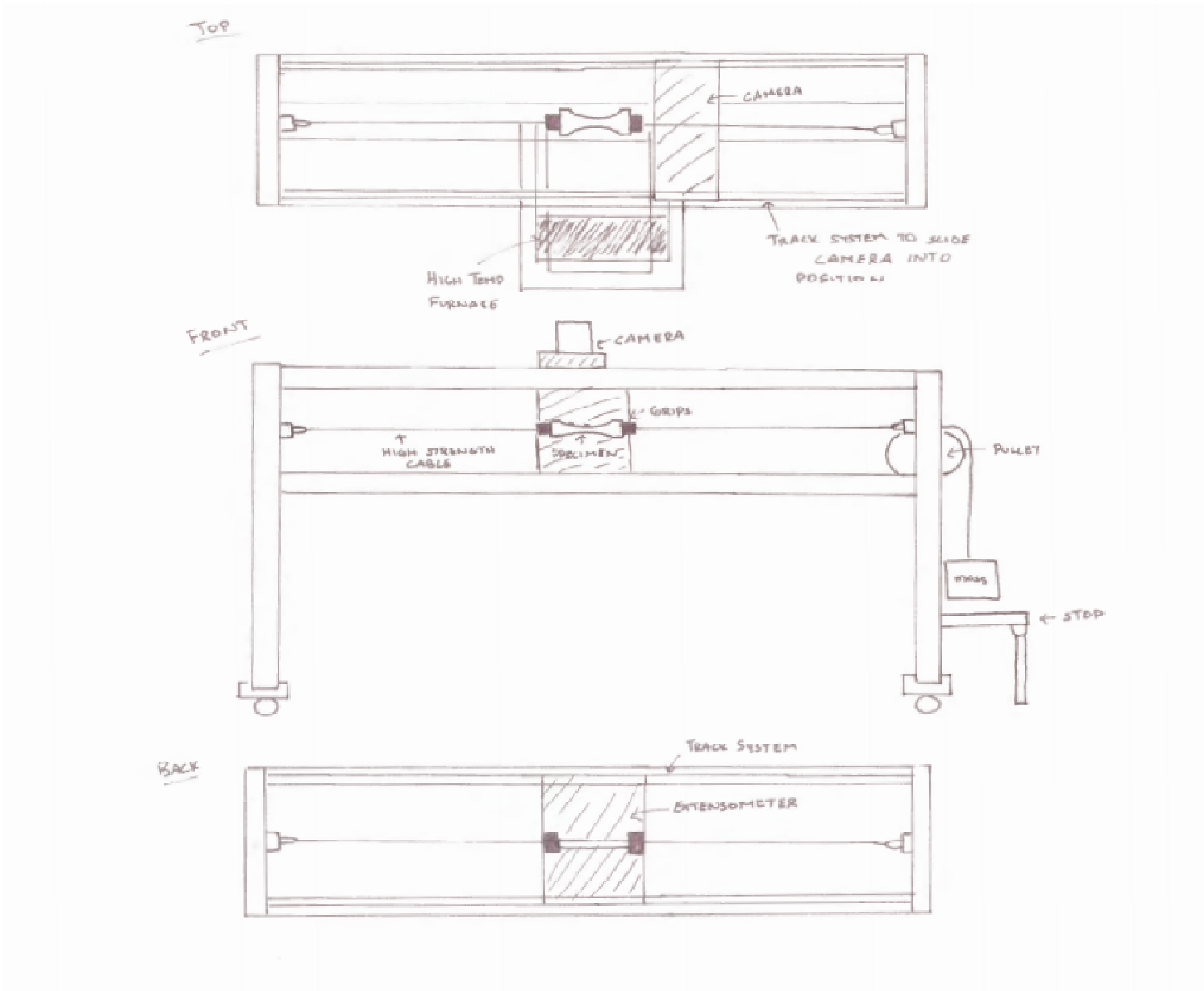

Figure 7. Third design sketch

This design moved the mass from the center of the frame to the side as well as implementing a track system for the camera, high temp furnace, and extensometer. The track system is implemented by making the frame out of aluminum structural framing. This design however, poses two problems. First, it does not satisfy the requirement that the specimen is pulled out of the furnace and then supported after rupture. Second, the light weight of the aluminum may not be enough to counterbalance the weight of the applied load without being additionally supported or fixed to the ground.

The next sketch is an attempt to solve both of the problems posed by the previous sketch. Figure 8 illustrates the design updates. The frame was changed from the aluminum structural framing to steel in order to provide additional weight and the test area was shortened to provide a stop for the specimen to pull out of the furnace after rupture.

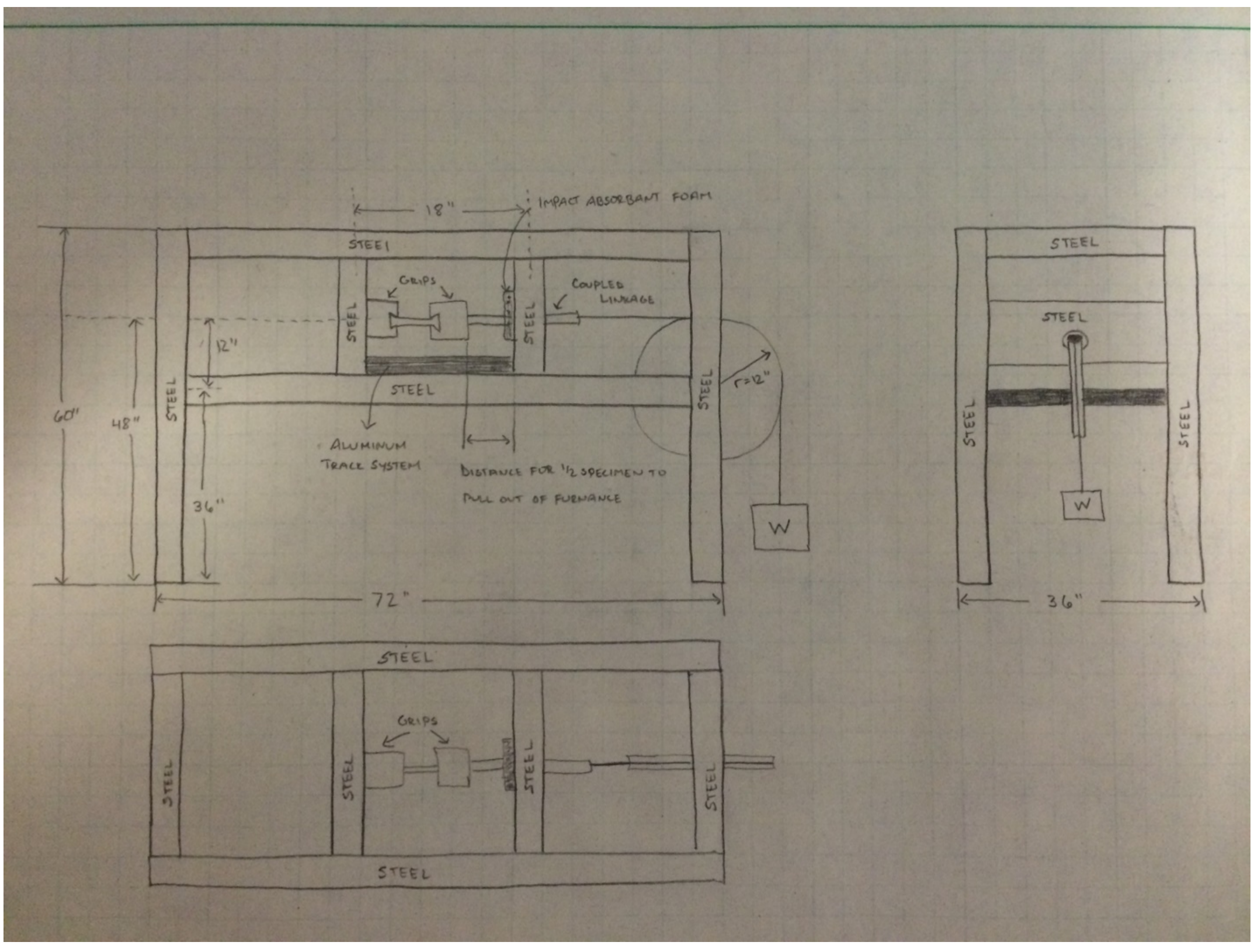

Figure 8. Fourth design sketch

In this design, the track system is added to the steel frame in order to provide for the additional test equipment. Once the test specimen ruptures, the weight is released and the specimen is pulled out of the furnace. A stop exists with an impact absorbent pad to protect the grip from contacting the steel structure. Since the test area has been shrunk to the middle of the frame, the additional weight from the structure outside the test area acts as a counterbalance. Because this sketch satisfies the design criteria it was chosen to move forward in the design process.

The critical points of the frame are where the maximum flexural stress and the maximum deflection will occur. For the current design, there are two components that will see the most stress and deflection. The first component is the beam that the left grip is attached to, and the second component is the rod that connects the pulley to the frame. The beam that the left grip is attached to is fixed at both ends as shown in figure 9.

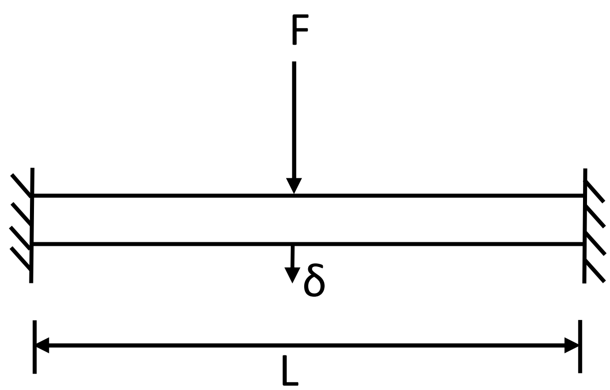

Figure 9. Fixed, Fixed beam

The maximum deflection of the beam will occur at L/2 and is given as

$$\delta_{MAX} = \frac{FL^3}{192EI} \tag{1}$$

where F is the force of the applied load, L is the length of the beam, E is the elastic modulus and I is the area moment of inertia. The maximum flexural stress will occur at the fixed ends of the beam and is given as

$$\sigma = \frac{FL}{8S} \tag{2}$$

where F is the force of the applied load, L is the length of the beam and S is the section modulus given as

$$S = \frac{bh^2}{6} \tag{3}$$

where b is the length and h is the height of the beam. The deflection and flexural stresses of the rod that the pulley is attached to are given by (1) and (2) respectively, but the area moment of inertia for a rod is

$$I = \frac{\pi}{4}r^4 \tag{4}$$

and the section modulus is

$$S = \frac{\pi}{4}r^3. \tag{5}$$

The derivations for (1) and (2) are shown in the appendix. A future study will be conducted in order to determine which material (aluminum structural framing or steel) is best suited for the frame design.

Grips for High Temperature Tensile Test

Gripping devices are used to transmit the load applied by the testing machine to the test specimen [1]. The grips for this design must be able to withstand the applied load and withstand high temperatures. Additionally, the grips will be designed for a contoured, edge-loaded test specimen as shown in Figure 10.

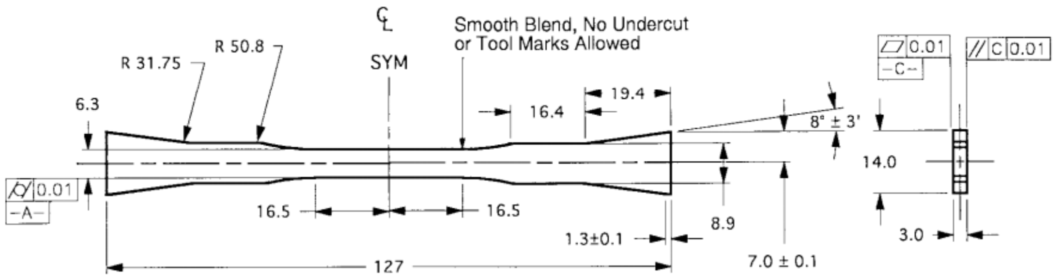

Figure 10. Contoured, Edge-Loaded Test Specimen Geometry [1]

Passive grip interfaces transmit the force applied by the test machine to the test specimen through a direct mechanical link [1]. Mechanical links utilize the geometrical features of the test specimen and uniform contact between the grip faces and the gripped section of the test specimen is crucial. Figure 11 shows an example of an edge-loaded, passive grip interface [1].

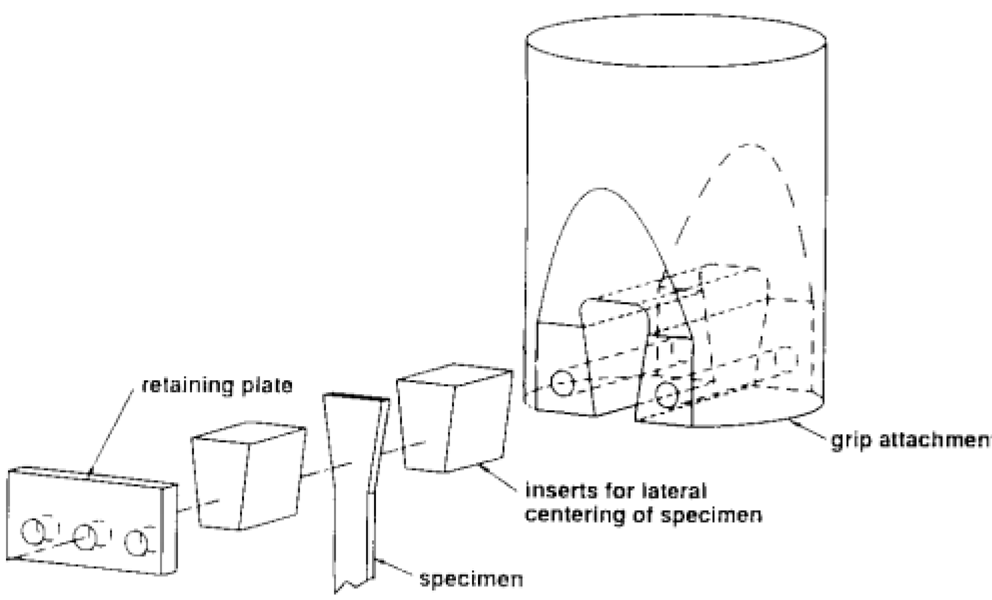

Figure 11. Edge-Loaded, Passive Grip Interface [1]

Material selection is very important in the design of the gripping devices. The material indices to be maximized in determining the ideal material for this application are $M_1 = \sigma_y$ (yield strength) and $M_2 = E$ (stiffness). In addition, the material must be able to withstand temperatures greater than or equal to 700 degrees Celsius and have a minimal thermal expansion coefficient. The material selection process also considers cost and manufacturing.

Using CES Selector, the material indices are defined and the materials that maximize performance (high strength and stiffness) are highlighted. Figure 12 displays the materials that maximize performance.

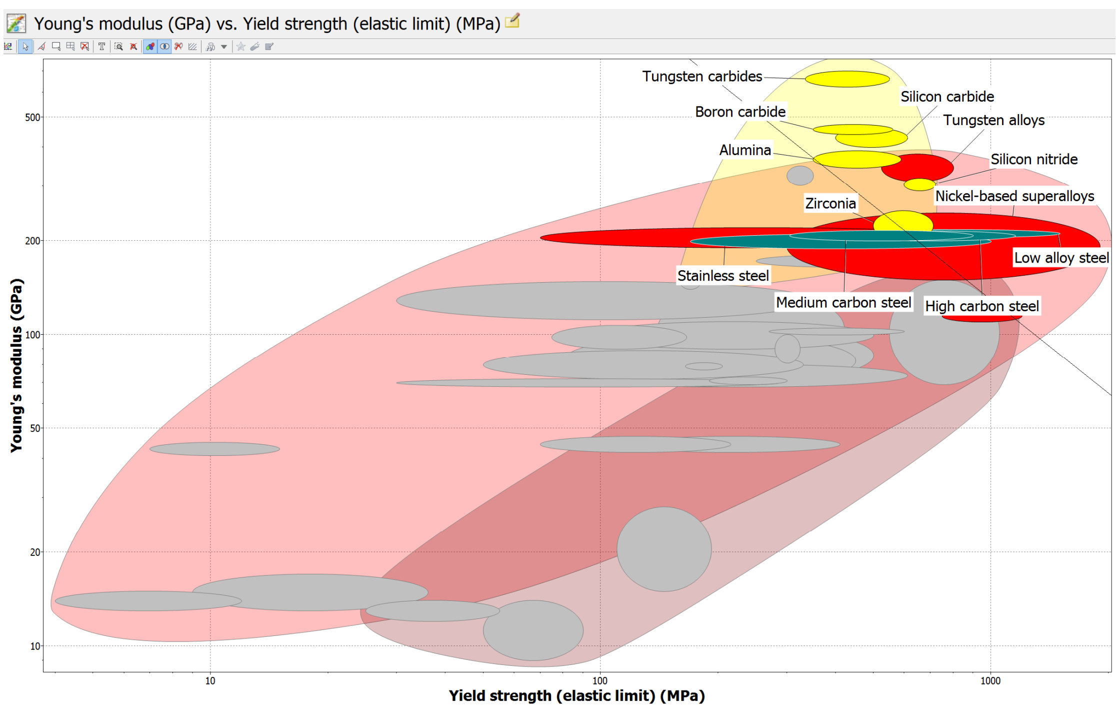

Figure 12. Performance graph: Young's modulus vs. Yield Strength

The performance graph shows that the best materials are technical ceramics such as: tungsten carbides, silicon carbide, silicon nitride, boron carbide, alumina, and zirconia, and metals such as: stainless steel, medium carbon steel, high carbon steel, low allow steel, and nickel-based superalloys.

In addition to high strength and high stiffness, the material used for the grips should be able to operate at temperatures higher than 700 degree Celsius. Adding this limit into the CES software eliminates medium carbon steel, and high carbon steel. Even though materials can withstand high temperatures, this does not imply that they have a low thermal expansion coefficient. The extent at which a material expands due to high temperatures should be minimized for this application and thus the ideal material will have a low thermal expansion coefficient. Figure 13 shows us that technical ceramics have a lower thermal expansion coefficient compared to metals and alloys.

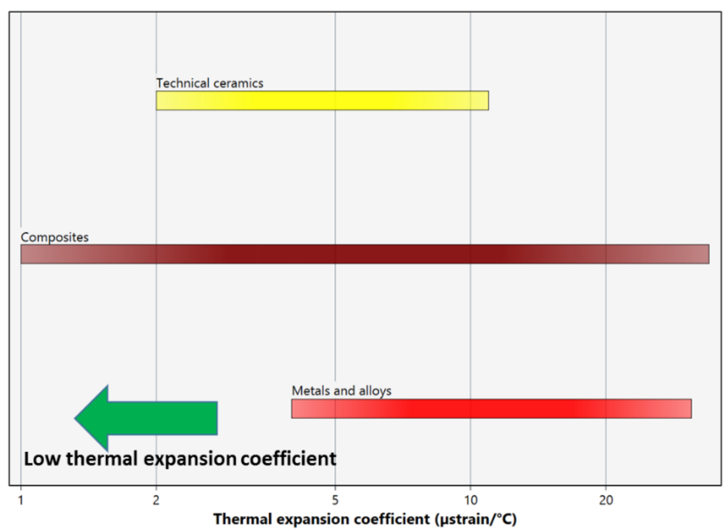

Figure 13. Thermal expansion coefficient

The ideal material for the grips seems to be a technical ceramic due to their great mechanical and thermal properties, but a cost and manufacturing process analysis must be performed before a final selection can be made.

Cost is extremely important in any material selection process. Cost is something that changes with time. Supply, scarcity, speculation, and inflation contribute to fluctuations in cost per kilogram of materials [2]. Performance is extremely important for this application; however, it is important to try and minimize cost whenever possible especially if performance doesn't suffer. Figure 14 shows the best materials with respect to price. Tungsten carbide, silicon carbide, stainless steel, and nickel-based superalloys are the top choices to minimize cost.

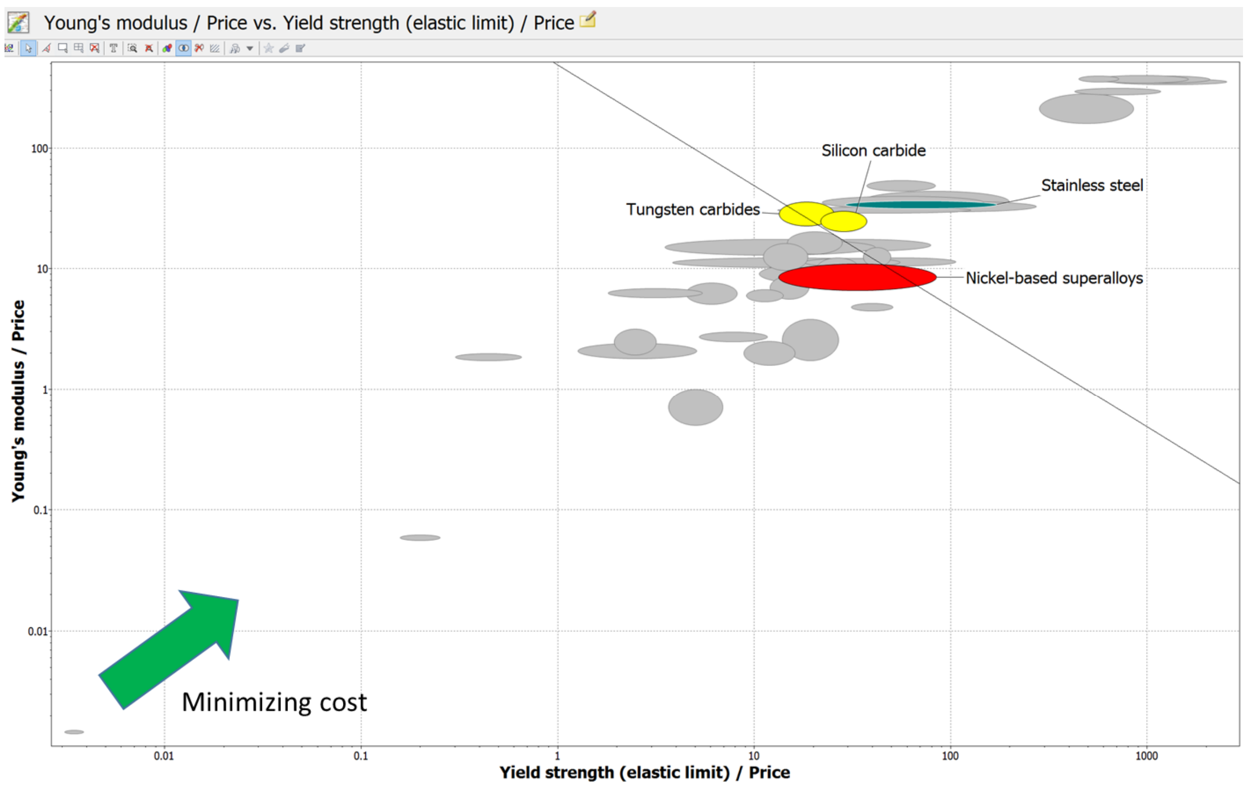

Figure 14. Cost analysis: Performance with respect to price

Stainless steel provides better strength with respect to price, but has a much higher thermal expansion coefficient. On the other hand, nickel-based superalloys have a lower stiffness compared to that of silicon carbide and tungsten carbides, but strength is more important than stiffness for this application so it remains as a possible material for this application. The material properties and price per kilogram of these four materials are compared and shown in Table 3.

	Silicon Carbide	Tungsten Carbides	Stainless Steel	Nickel-based super alloys
Yield Strength (MPa)	500	443	585	900
Tensile Strength (MPa)	500	460	480	600
Stiffness (GPa)	530	663	200	198
Thermal Expansion Coefficent (μstrain/°C)	4.4	6.15	17	13
Max Service Temperature (°C)	1550	875	785	1050
Hardness (HV)	2450	2900	350	400
Fracture Toughness (Mpa.m$^{0.5}$)	4.3	2.9	106	85
Price per kg ($/kg)	$17.60	$23.85	$5.86	$22.55

Table 3. Material properties and price per kg

From Table 3, tungsten carbides are eliminated from the selection process since the objective is to minimize cost and tungsten carbides cost the most per kilogram. Nickel-based superalloys have great yield and tensile strength but have poor stiffness in comparison to that of silicon carbide. Silicon carbide has great strength and stiffness properties as well as a low thermal expansion coefficient and excellent hardness. Hardness is important for this application because the grip will impact the stop once the specimen ruptures. Since the yield strength and tensile strength of silicon carbide is more than sufficient for this application we can eliminate nickel-based superalloys due to the comparison with silicon carbide and the fact that silicon carbide is cheaper. Stainless steel meets the service temperature requirement and has good yield and tensile strength so it remains only as an economical choice due its low cost per kilogram; however, overall performance suffers in comparison with silicon carbide.

Based on this analysis, silicon carbide is the ideal material for this application. Performance is extremely important for a creep testing machine because it must be able to accurately represent the true creep of the material.

Now that a material has been selected, it is important to determine the best shaping process for the material. Figure 15 shows the process-material compatibility matrix and we can see that we have three possible processes available for ceramics: powder methods, electro-machining, and conventional machining. Powder methods are economically beneficial only for large batch sizes and electro-machining is ideal for very good conductors. Since the design includes two grips and silicon carbide is a semi-conductor, the conventional machining of the grips will be appropriate.

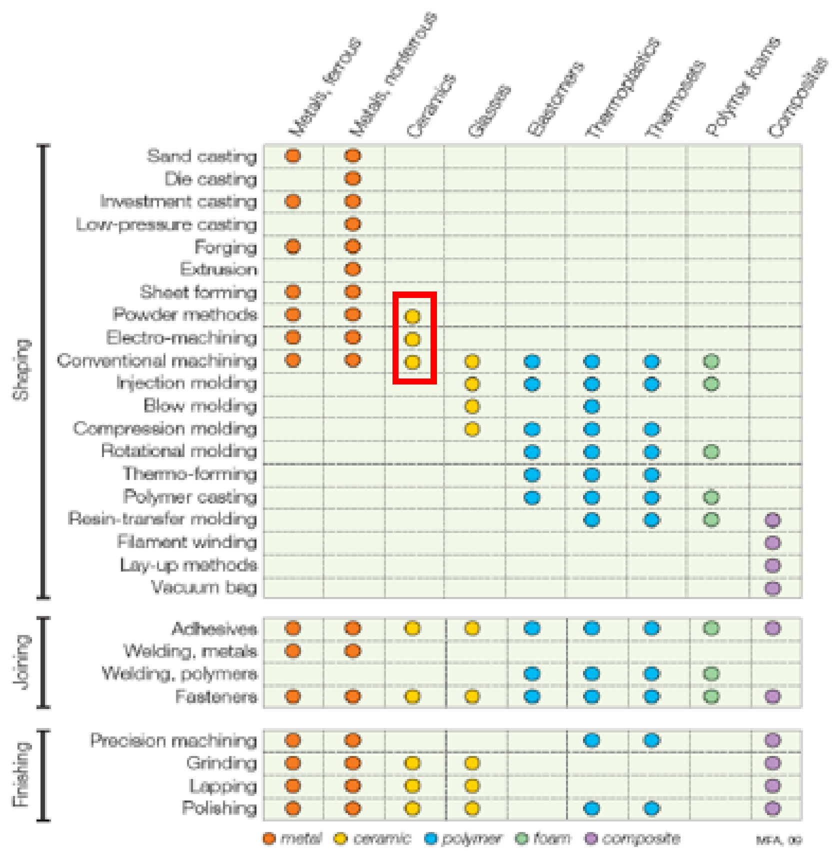

Figure 15. Process-Material Compatibility Matrix

Conclusion

With a final design to move forward with, the next step is to develop a comparison between the aluminum structural framing and steel. The goal of this analysis will be to see which material is better suited to withstand the applied load and the resulting moment that will be created. The aluminum structural framing is the preferred material due to its t-slotted modular profile which would be utilized as the track system. After this analysis is complete, a preliminary CAD drawing can be made and structural simulations can be performed to see how the frame performs under the applied load.

The material selection process is completed for the grips and the next step is to design the grips for the contoured-edge loaded test specimen geometry as shown in Figure 10. Once the grips are designed, manufacturing can begin.

Overall, the design for the horizontal creep test is moving forward and further work will continue to take this proof of concept to the manufacturing stage.

References

[1] Standard Test Method for Monotonic Tensile Behavior of Continuous Fiber-Reinforced Advanced Ceramics with Solid Rectangular Cross-Section Test Specimens at Ambient Temperature. ASTM C 1275 – 00.

[2] Ashby, Michael, F. 2011. Materials Selection in Mechanical Design. Fourth Edition. Kidlington, Oxford: Elsevier Ltd.

Appendix

DERIVATION FOR MAXIMUM DEFLECTION

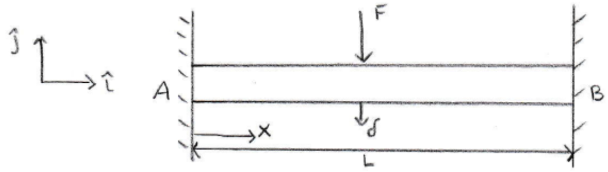

FBD

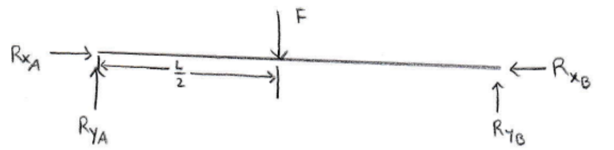

$$\xrightarrow{+} \sum F_x = 0 = R_{x_A} - R_{x_B}$$

$$\Rightarrow R_{x_A} = R_{x_B}$$

$$\uparrow + \sum F_y = 0 = R_{y_A} + R_{y_B} - F$$ (DUE TO SYMMETRY OF BOTH THE LOADING AND GEOMETRY $\Rightarrow R_{y_A} = R_{y_B}$)

$$\Rightarrow R_{y_A} = R_{y_B} = \frac{F}{2}$$

$x_1 < \frac{L}{2}$

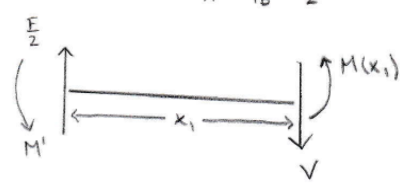

SYMMETRY $\Rightarrow$ MOMENT AT A AND MOMENT AT B ARE EQUAL

$$\curvearrowleft + \sum M = 0 = M(x_1) - \frac{F}{2}x_1 + M'$$

$$M(x_1) = \frac{F}{2}x_1 - M'$$

$$EI\frac{d^2v}{dx_1^2} = M(x_1)$$

$$\Rightarrow EI\frac{d^2v}{dx_1^2} = \frac{F}{2}x_1 - M'$$

$$\Rightarrow EI\frac{dv}{dx_1} = \frac{F}{4}x_1^2 - M'x_1 + c_1 \quad \text{— (1)}$$

$$\Rightarrow EIv = \frac{F}{12}x_1^3 - \frac{M'}{2}x_1^2 + c_1x_1 + c_2 \quad \text{— (2)}$$

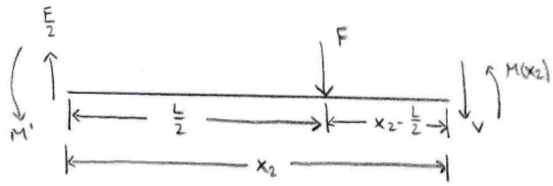

$$\circlearrowleft \sum M = 0 = M(x_2) - \frac{F}{2}x_2 + F\left(x_2 - \frac{L}{2}\right) + M'$$

$$\Rightarrow M(x_2) = \frac{F}{2}x_2 - Fx_2 + \frac{FL}{2} - M'$$

$$EI\,\frac{d^2v}{dx_2^2} = M(x_2)$$

$$\Rightarrow EI\,\frac{d^2v}{dx_2^2} = \frac{F}{2}x_2 - Fx_2 + \frac{FL}{2} - M'$$

$$\Rightarrow EI\,\frac{dv}{dx_2} = \frac{F}{4}x_2^2 - \frac{F}{2}x_2^2 + \frac{FL}{2}x_2 - M'x_2 + c_3 \quad - (3)$$

$$\Rightarrow EIv = \frac{F}{12}x_2^3 - \frac{F}{6}x_2^3 + \frac{FL}{4}x_2^2 - \frac{M'}{2}x_2^2 + c_3x + c_4 \quad - (4)$$

BOUNDARY CONDITIONS @ x_1

$$v'(0) = 0$$

$$v(0) = 0$$

FROM (1) $\Rightarrow c_1 = 0$

(2) $\Rightarrow c_2 = 0$

IF $x_1 = x_2 = \frac{L}{2} \Rightarrow v'(x_1) = v'(x_2)$

$$\Rightarrow c_3 + \frac{F}{4}\left(\frac{L}{2}\right)^2 - \frac{F}{2}\left(\frac{L}{2}\right)^2 + \frac{FL}{2}\left(\frac{L}{2}\right) - M'\left(\frac{L}{2}\right) = \frac{F}{4}\left(\frac{L}{2}\right)^2 - M'\left(\frac{L}{2}\right)$$

$$\Rightarrow c_3 = \frac{FL^2}{8} - \frac{FL^2}{4} = \frac{-FL^2}{8}$$

IF $x_1 = x_2 = \frac{L}{2} \Rightarrow v(x_1) = v(x_2)$

$$\Rightarrow c_4 + \frac{F}{12}\left(\frac{L}{2}\right)^3 - \frac{F}{6}\left(\frac{L}{2}\right)^3 - \frac{FL}{4}\left(\frac{L}{2}\right)^2 - \frac{M'}{2}\left(\frac{L}{2}\right)^2 - \frac{FL^2}{8}\left(\frac{L}{2}\right) = \frac{F}{12}\left(\frac{L}{2}\right)^3 - \frac{M'}{2}\left(\frac{L}{2}\right)^2$$

$$\Rightarrow c_4 = \frac{FL^3}{48} + \frac{FL^3}{16} - \frac{FL^3}{16} = \frac{FL^3}{48}$$

$$EIv = \frac{F}{12}x_2^3 - \frac{F}{6}x_2^3 + \frac{FL}{4}x_2^2 - \frac{M'}{2}x_2^2 - \frac{FL^2}{8}x_2 + \frac{FL^3}{48}$$

$v(L) = 0$

$$\Rightarrow 0 = \frac{FL^3}{12} - \frac{FL^3}{6} + \frac{FL^3}{4} - \frac{M'}{2}L^2 - \frac{FL^3}{8} + \frac{FL^3}{48}$$

$$\Rightarrow \frac{M'}{2}L^2 = \frac{FL^3}{16}$$

$$\Rightarrow M' = M_A = M_B = \frac{FL}{8}$$

$$\Rightarrow EIv = \frac{-FL}{12}x^3 + \frac{3FL}{16}x^2 - \frac{FL^2}{8}x + \frac{FL^3}{48}$$

MAXIMUM DEFLECTION AT $x = \frac{L}{2}$

$$\Rightarrow EIv_{MAX} = \frac{-FL^3}{96} + \frac{3FL^3}{64} - \frac{FL^3}{16} + \frac{FL^3}{48}$$

$$\Rightarrow EIv_{MAX} = \frac{-FL^3}{192}$$

$$\Rightarrow v_{MAX} = \frac{-FL^3}{192EI}$$

(NEGATIVE SIGN IMPLIES DEFECTION OCCURS IN $-\hat{j}$ DIRECTION)

IRRESPECTIVE OF DIRECTION

$$\Rightarrow \boxed{\delta_{MAX} = \frac{FL^3}{192EI}}$$

DERIVATION FOR STRESS AT CRITICAL POINTS

$$\sigma = \frac{Mc}{I}$$

SECTION MODULUS $\rightarrow$ $S = \frac{I}{c}$; FROM DERIVATION FOR MAXIMUM DEFLECTION, MOMENT AT ENDS, $M_A = M_B = \frac{FL}{8}$

$$\Rightarrow \boxed{\sigma = \frac{FL}{8S}}$$